Understanding the Mechanism and Regio-and Stereo selectivity of [3+2] Cycloaddition Reactions between Substituted Azomethine ylide and 3,3,3-Trifluoro-1-nitroprop-1-ene, within the Molecular Electron Density Theory

Chafia Sobhi, Lynda Merzoud, Souad Bouasla, Abdelmalek Khorief Nacereddine, Christophe Morell, Henry Chermette

Understanding the Mechanism and Regio- and Stereo selectivity of [3+2] Cycloaddition Reactions between Substituted Azomethine ylide and 3,3,3-Trifluoro-1-nitroprop-1-ene, within the Molecular Electron Density Theory

Chafia Sobhi[a], Lynda Merzoud[b], Souad Bouasla[c], Abdelmalek Khorief Nacereddine[d], Christophe Morell[b] and Henry Chermette[b]

[a]Laboratoire Physico-Chimie Des Surfaces Et Interfaces, Université du 20 Août1955, B.P 26 Skikda 21000, Algeria

[b]Université de Lyon, Université Claude Bernard Lyon 1,Institut des Sciences Analytiques, UMRCNRS 5280, 69622 Villeurbanne Cedex, France

[c]Laboratory of Materials and Energetic Engineering, Faculty of Technology, University 20August 1955 Skikda, BP 26, 21000, Skikda, Algeria

[d]Laboratory of Physical Chemistry and Biology of Materials, Department of Physics and Chemistry, Higher Normal School for Technological Education of Skikda,Azzaba, Skikda, Algeria

Abstract

The selectivity and the nature of the molecular mechanism of the [3+2] cycloaddition (32CA) reaction between2-(dimethylamino)-1H-indene-1,3(2H)-dione (**AY11**) and trans(E)-3,3,3-trifluoro-1-nitroprop-1-ene(**FNP10**) has been studied, in which the Molecular Electron Density Theory (MEDT) using DFT methods at the MPWB1K/6-31G(d) computational level was used. Analysis of the global reactivity indices permits us to characterize **FNP10** as a strong electrophile and **AY11** as a strong nucleophile. Four reactive pathways associated with the *ortho*/*meta* regioselective channels and *endo*/*exo* stereoselective approaches modes have been explored and characterized in the gas phase and in the benzene solvent. The analysis of the relative energies associated with the different reaction pathways indicates that the 32CA reactions of the azomethine ylide (**AY)** with the nitroalkene (**FNP**) is *meta* regioselective with high *endo* stereoselectivity. This result is in good agreement with the experimental

observations. ELF topological analysis of the most favored reactive pathways allows for characterizing the mechanism of this 32CA reactions as a non-concerted *two-stage one-step* mechanism. Finally, non-covalent interactions (NCIs) and QTAIM analyses at the *meta/endo* transition state structure indicate that the presence of different several weak interactions, namely, C−F and N−H contributed in favoring the formation of a *meta-endo* cycloadduct.

Keywords: Azomethine ylide; Nitroalkene; [3 + 2] Cycloaddition; Selectivity; MEDT; Mechanism; DFT Calculations.

1. INTRODUCTION

The [3+2] cycloaddition (32CA) reactions are among the most important and commonly used strategy in biological, materials, and drug chemistry. This reaction is used to build five membered heterocycles in a single preparative step, leading to the formation of up to four stereogenic centres.[1-3] It involves the addition of a three-atom-component (TAC) like azides, nitrones, carbonyl ylides, nitrile oxides, nitrile imines and azomethine ylides to an ethylene derivative.[4] In particular, the cycloaddition of azomethine ylides with alkenes, to generate pyrrolidines, pyrrolizidines, spiropyrrolidines, and spiropyrrolizidines, which are key synthons that are found in a variety of natural products.[5] Those products display a wide spectrum of biological activities, *i.e.* antibacterial, cytotoxicity, [6] histamine H3-receptor ligands,[7] antifungal,[8] anticancer,[9] and cholinesterase inhibitors.[10] In this regard, much attention has been paid to the development of efficient methodologies for the preparation of structurally diverse spiro compounds. The rationalization of the different outcomes and the nature of the reaction mechanisms are still the subject of different recent studies. Thus, a considerable amount of Molecular Electron Density Theory (MEDT) studies have been devoted to understand the reactivity and the regioselectivity of 32CA reactions involved azomethine ylides. However, the result of each new reaction is not necessarily obvious.[11]

A recent MEDT study of the 32CA reaction of a chiral azomethine ylide (AY) with β-nitrostyrene (NS) has been performed using DFT methods at the MPWB1K/6-31G(d) computational level. [12] The authors showed that the reaction proceeds *via* a polar mechanism, and present a relatively low activation enthalpy of 4.1 kcal/mol in which the *meta/endo* cycloadduct is formed as a major product (Scheme 1).

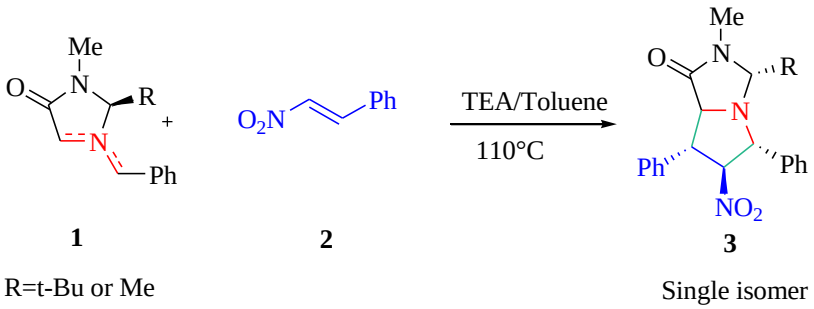

Scheme 1. 32CA reactions between azomethine ylide **1** with β‑nitrostyrene **2**

Recently, Essam M *et al*. [13] reported an experimental and theoretical study to facilitate the synthesis of functionalized di-spiro[indoline-3,2′-pyrrolidine-3′,3″-indolines] *via* a one-pot TAC 32CA reaction of the sarcosine and (E)-3-(2-oxo-2-(pyren-1-yl) ethylidene) indolin-2-one derivatives. This 32CA reaction can yield the formation of the corresponding cycloadducts (CAs) which is characterized by a complete regioselectivity (Scheme 2). For this, the authors investigate different theoretical methods such as, density functional theory (DFT) using the B3LYP/6-31G(d) basis set and the corresponding conceptual density functional theory (CDFT) of the reactants in order to explain the molecular mechanism and the selectivity of these cycloaddition reactions.

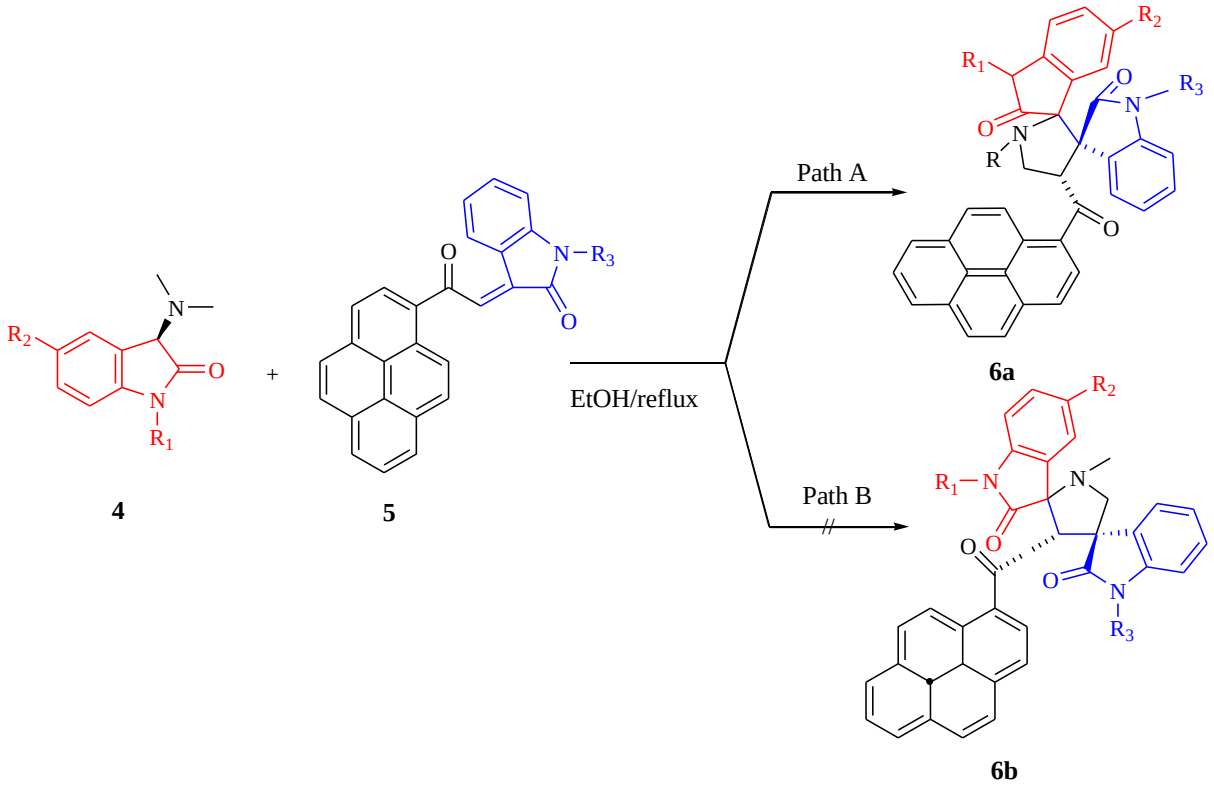

Scheme 2. 32CA of sarcosine and (E)-3-(2-oxo-2-(pyren-1-yl) ethylidene) indolin-2-one derivative

More recently, Wang et *al.*[14] realized a detailed theoretical study using DFT method to investigate the mechanism of the 32CA reaction between (Z)-1-methyl-3-[(2,2,2-trifluoroethyl)imino]indolin-2-one **7** and 5-nitro-2-vinylpyridine **8** (Scheme 3). In their study, the authors reveal that the most favored reaction pathway proceeds via three steps, in which the first and the second steps are the proton transfer reactions, whereas, the third step is the 32CA reaction (Scheme 3).

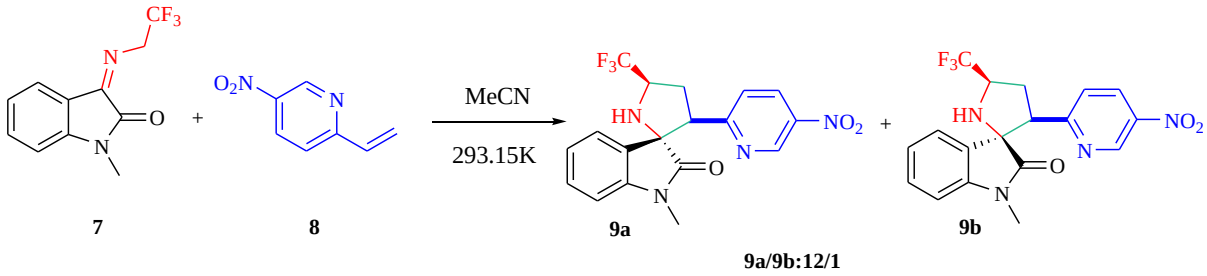

Scheme 3. 32CA reactions between azomethine ylide 7 and 5-nitro-2-vinylpyridine 8

Alexey *et al.* [15] reported the synthesis of numerous types series of spiroindene pyrrolidines and spiroindene pyrrolizidines using the cycloaddition reactions of (*E*)-3,3,3 trihalogeno-1-nitropropenes with stabilized azomethine ylides to derived ninhydrin and indenoquinoxalinones under mild experimental conditions (Scheme 4). They have found that this 32CA reaction is regio- and stereoselective yielding to the formation of the corresponding *meta/endo* cycloadduct as a major synthon in all reactions.[15]

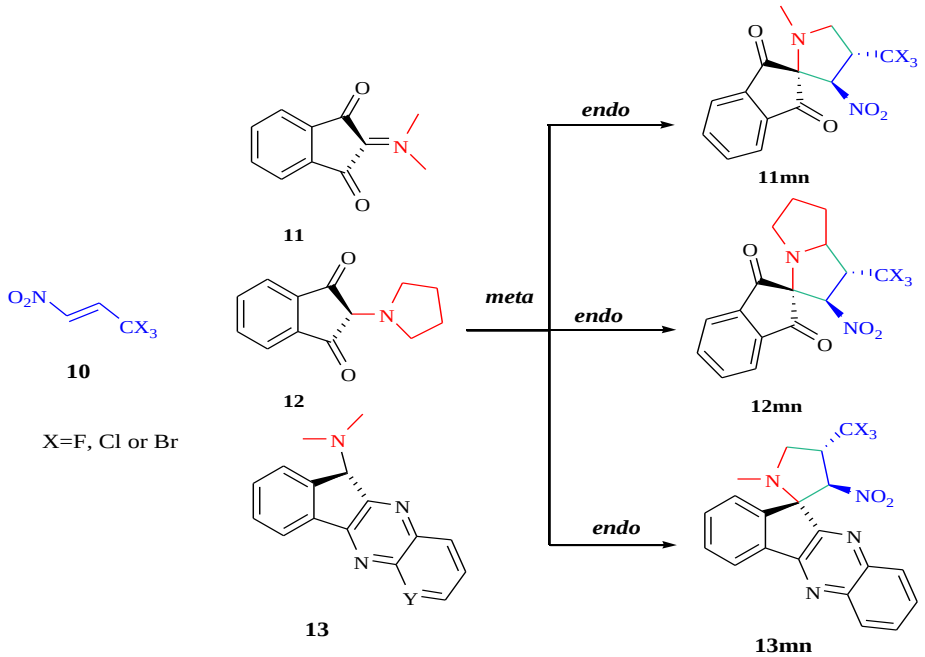

Scheme 4. 32CA reactions of (E)-3,3,3 trihalogeno-1-nitropropenes with stabilized azomethine ylides

Over the last years, theoretical chemists have attached great importance to the study and analysis of the nature and mechanism of chemical reactions in order to predict the selectivity of molecules before and during the reaction course. An attempt to explain the mechanistic behaviours of organic reactions, since the first appearance of the model proposed by Houk [16] which depends mainly on the interaction between the frontier molecular orbitals (FMO), and lately, the modern Domingo's molecular electron density theory (MEDT), [17] which focuses on the change of electron density during the approach of reactants.

In order to follow our previous works, toward the investigation of molecular mechanism of the 32CA reactions [18], we have realized a MEDT study of the regio- and stereoselectivities, experimentally observed in the 32CA reaction of azomethine ylide (**AY11**) with(E)-3,3,3-trifluoro-1-nitroprop-1-ene (**FNP10**) (Scheme5) using the MPWB1K/6-31G(d) computational level. The main goal of the present study is to get insight on the factors controlling the reactivity and selectivity of this 32CA reaction.

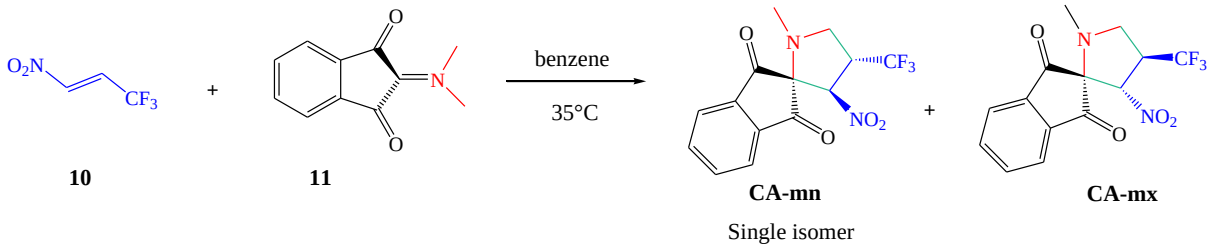

Scheme 5. 32CA reaction between **AY11** and (E)-3,3,3-trifluoro-1-nitroprop-1-ene **FNP10**

2. COMPUTATIONAL METHODS

All stationary points involved in these 32CA reactions were optimized using the MPWB1K functional[19] together with the 6-31G(d) basis set.[20] This functional was selected because it is accurate for kinetic data and provides a good thermodynamic outcome[12, 21] and gave the best results among a set of functionals (see Supporting Information table S1, S2). The optimizations were carried out using the Berny analytical gradient optimization method.[22] The stationary points were characterized by frequency computations in order to verify that TSs have one and only one imaginary frequency. The IRC paths[23] were plotted in order to check that the energy profiles connect each TS to the two associated minima of the proposed mechanism using the second order González-Schlegel

integration method.[24] Solvent effects of benzene were taken into account through single point energy calculations using the polarizable continuum model (PCM) developed by Tomasi *et al.*[25] in the framework of the self-consistent field reaction.[26, 27, 28] Values of enthalpies, entropies, and Gibbs free energies in benzene were calculated at 308 K and 1 atm over the optimized gas phase structures[29] and based on the vibrational frequencies scaled by 0.96.[30] The global electron density transfer (GEDT) at the TSs was computed by the sum of the natural atomic charges, obtained through a natural population analysis (NPA) of the atoms building each one of the separated reagents.[31] The electronic structures of the TSs were analyzed by the natural bond orbital method (NBO). The electron localization function (ELF) [32] was performed using the Multiwfn software [33] from the MPWB1K /6–31G(d) monodeterminantal wave functions of the selected points at the IRC diagram. All calculations were performed using Gaussian 09 package.[34]

The global electrophilicity index ω [35] is given by the following expression, $w = (m^2 / 2h)$ in terms of the electronic chemical potential μ and the chemical hardness η. Both quantities may be approached in terms of the one-electron energies of the frontier molecular orbitals HOMO and LUMO, ε_H and ε_L, as $\mu = (\varepsilon_H + \varepsilon_L)/2$ and $h \approx (e_L - e_H)$, respectively.[36] The empirical (relative) nucleophilicity index *N*, [37, 38] based on the HOMO energies obtained within the Kohn-Sham scheme[39] is defined as $N = \varepsilon_{HOMO\ (Nu)} - \varepsilon_{HOMO(TCE)}$, where TCE is tetracyanoethylene. TCE is the reference because it presents the lowest HOMO energy in a long series of molecules already investigated in the context of polar organic reactions. Non covalent interactions (NCIs) analysis was performed by evaluating the reduced density gradient and low- gradient isosurface.[40-42] Quantum theory of atoms in molecule (QTAIM) analysis [43] was performed with the Multiwfn program [33] using the corresponding MPWB1K /6-31G(d) monodeterminantal wave functions.

3. RESULTS AND DISCUSSIONS

The present MEDT study has been divided into four parts: (*i*) the first is devoted to the analysis of the DFT reactivity indices of the reagents involved in the CA reaction of **AY11** with **FNP10**, in order to determine the electronic character of the reagents at the ground states; (*ii*) in the second part, the potential energy surfaces associated with the four competitive channels in the 32CA reaction of **AY11** with**FNP10** will be analyzed and discussed, in terms of relative electronic energies, enthalpies, together with the GEDT. In the

third part, (*iii*) an ELF topological analysis focused on the formation of the C1−C4 and C3−C5 single bonds along the most favorable *meta/endo* reactive channel of the 32CA reaction between **AY11** and **FNP10** is performed. Finally, the NCI gradient isosurfaces and QTAIM parameters were performed in order to discern the origin of the experimentally observed high *endo-meta* selectivity of this 32CA reaction.

3.1. Conceptual DFT indices

Previous studies devoted to Diels-Alder and 32CA reactions have shown that the conceptual DFT (CDFT) indices [44, 45] are powerful tools which can be used to understand the reactivity in polar cycloadditions. The chemical reactivity indices, namely, electronic chemical potentialμ, chemical hardness η, global electrophilicity ω, and global nucleophilicity *N*, of the separated reagents, **AY11**and**FNP10** are given in Table 1.

Table 1. Electronic chemical potential μ, chemical hardness η, global electrophilicity ω, and global nucleophilicity N, indices of **AY11**, and **FNP10** calculated at B3LYP/6-31G(d) level are given in eV

	HOMO	LUMO	μ	η	ω	N
AY11	-5.653	-1.936	-3.79	3.72	1.94	3.47
FNP10	-8.533	-3.261	-5.90	5.27	3.30	0.59

Commonly, polar cycloaddition reactions are characterized by an electron density transfer from the nucleophilic species toward the electrophilic ones. This electron density transfer is measured by the global electron density transfer (GEDT)value at the TSs, in which the polar reactions have been characterized by a large value of GEDT.[31] Recently, Domingo *et al.* found a good correlation between the polar character of the cycloaddition reactions and their activation energies and consequently their feasibility.[46] Thus, in our case (see Table 1), a comparison between the electronic chemical potential (μ) values shows that the**AY11** present a value (μ = −3.79 eV) higher than that of **FNP10**(μ = −5.79 eV). These values suggest that along this polar 32CA reaction, the GEDT will flow from **AY11** toward **FNP10**. Thus, this 32CA reaction is classified as the forward electron density flux (FEDF), [47] which correlates well with the GEDT analysis performed at the TSs (vide infra).

Currently, polar cycloaddition reactions involve the participation of both good electrophiles and good nucleophiles, therefore the use of multiple substitutions with electron-withdrawing (EW) groups accelerates the cycloaddition with the increase of the electrophilic character of the ethylene. However, the presence of the nitro group in the electrophile contributes as an

electron withdrawing group and makes it a good electrophile. Fortunately, the inclusion of the trifluoro group at the β-position of the nitroethylene framework markedly increases the reactivity of nitroethylene as an electrophile (It acts through an inductive effect, -I), but it does not modify its strong selectivity in 32CA reactions,[45] however, the presence of two nucleophile groups increase the electrophilicity value of alkene **FNP10, ω =3.30 eV**, and making it possible to classify this species as strong electrophile on the electrophilicity scale.[48]

In addition, **AY11** has a moderate electrophilicity value, ω=1.94 eV, being classified as a moderate electrophile. However, it presents a high nucleophilicity value, with *N*=3.47 eV, allowing for its classification as a strong nucleophile.[49] Consequently, the strong nucleophilic character of **AY11** and the strong electrophilic character of disubstituted ethylene account for the feasibility of this 32CA reaction with very low activation energy (see later).

3.2. Energies and geometries

Owing to the asymmetry of the reagents, the 32CA reaction between these entities could yields two pairs of regioisomeric and stereoisomeric CAs (see Scheme 6). The formation of these CAs can be related to the *endo* and *exo* stereoisomeric approaches of the nitro group of **FNP10** relative to the nitrogen atom of **AY11.** The two regioisomeric *meta* and *ortho* channels are associated with the formation of the C_1–C_4 and C_3–C_5 single bonds. The experimental results indicate that this 32CA reaction is characterized by a *meta* regioselectivity, in which the *endo* approach is more favored than the *exo* one[15].

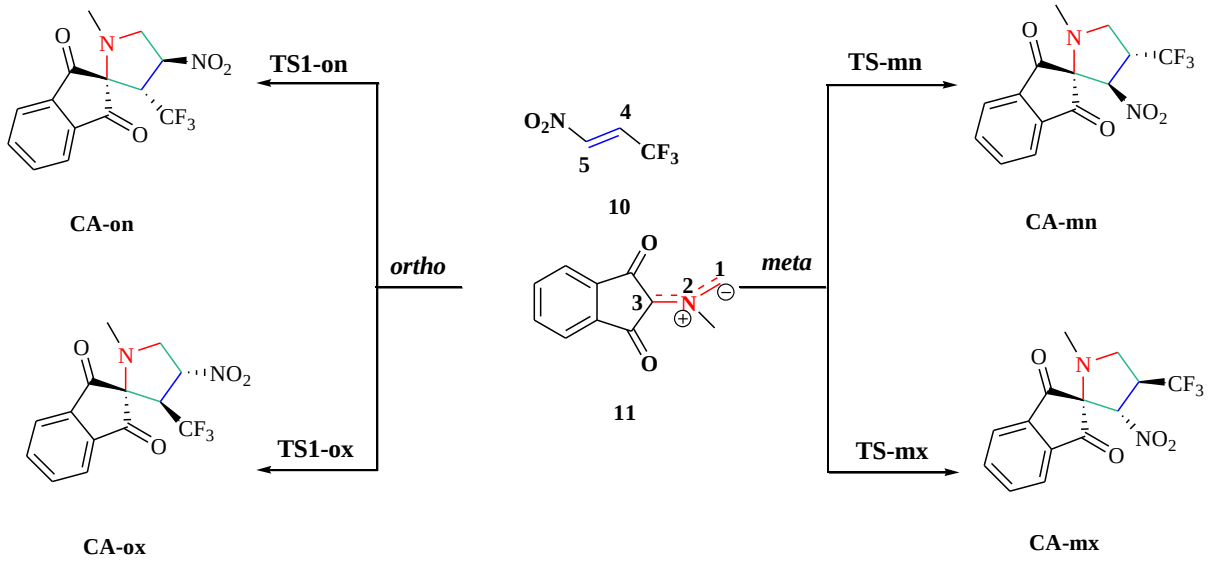

Scheme 6. The possible regio- and stereoisomeric pathways for the 32CA reaction of **AY11**with**FNP10**

The analysis of IRC paths associated to this 32CA reaction indicated that it takes place *via* a *one-step* mechanism (see Figure S1 in supplementary information). The relative energy values calculated with the MPWB1K of the stationary points associated with this 32CA reaction in gas phase and in benzene are summarized in Table 2, whereas the total ones are collected in Table S3 in the Supporting Information. The relative energy profiles for the four completive pathways are depicted in Figure 1.

The calculated activation energies are 5.14, 7.51, 7.99, and 8.99kcal/mol for **TS-mn**, **TS-mx**, **TS-on**, and **TS-ox**, respectively, however, when the formation of the molecular complex MC-mn is considered, the activation energy of this 32CA reaction becomes positive at 5.14 kcal/mol. These energy results indicate that the *meta* regioisomeric approach mode is more favorable than the *ortho* one. Also, **TS-mn** activation energy is lower than **TS-on** by 2.85 kcal/mol, indicating that the *meta*/*endo* reactive pathway is kinetically more favorable than the *meta/exo* one. Consequently, this 32CA reaction is total regio- and stereoselective, leading underkinetic control to favor theformation of **CA-mn** cycloadduct. This result is in good agreement with the experimental outcome, in which the **CA** generated from *meta-endo* approach was obtained as a single isomer. [15]In addition, the relative energies of cycloadducts are very negative, ranging from -52.49(**TS-ox**) to -57.27 (**TS-mx**) kcal/mol., accounting for the irreversibility of this 32CA reaction, and indicates that is only under kinetic control.

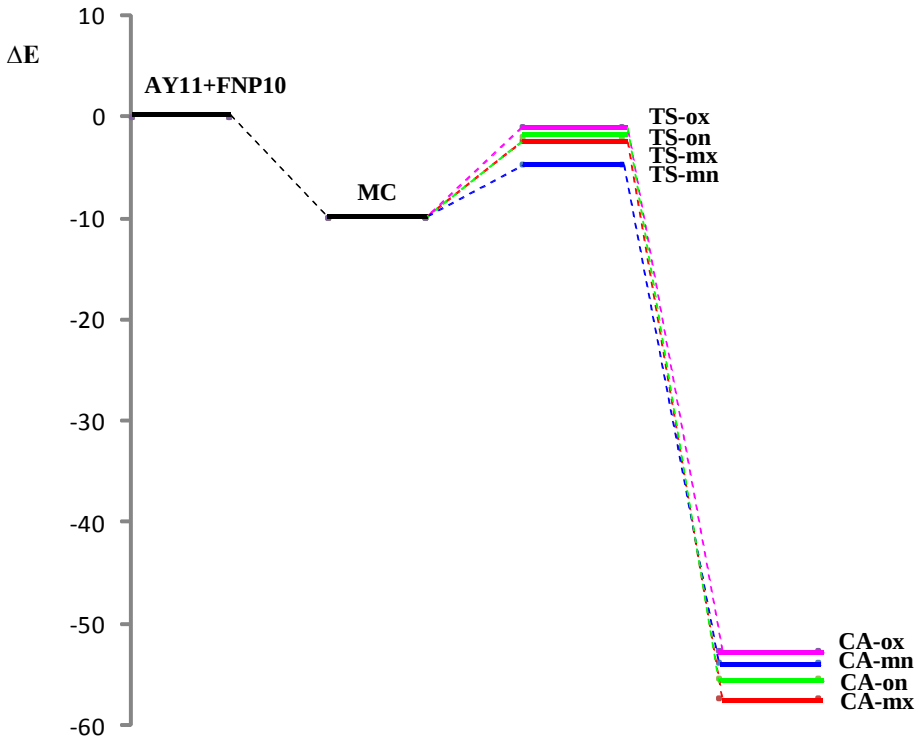

Figure 1. Relative energy profile of the pathways associated with the 32CA reaction of azomethine ylide **11** with alkene **10**

Since the major amount of organic reactions were realized in solution, herein the 32CA reaction of **AY11** with (E)-3,3,3-trifluoro-1-nitroprop-1-ene**10** is carried out in a low polar solvent (benzene ε=2.27), and it can have some influence on the energies. The optimized structures obtained in the gas phase were used through single-point energy calculations to take into account the solvent effects of benzene. The relative energy results are summarized in Table 2 while the total ones are gathered in Table S3 in supporting information. From Table 2, we can observe an increase in the activation energies and a decrease of the exothermic character of this 32 CA reaction, which may be due to the fact that the solvent effects stabilize reactants effectively **AY11** and **FNP10** more than TSs and CAs, as a consequence of the higher solvation of the reactants in low polar solvents.[50] In addition, although the increasing of relative energies between 0.84 and 1.29 kcal·mol^{-1}, the selectivity does not noticeably modified, in which the *meta/endo* approach remains the most favorable reactive channel, in good agreement with the gas-phase study and experimental data.[15]

Table 2. Relative energies (to [**AY11**+ alkene**10**], in kcal·mol^{-1}), in gas phase and in benzene, of the stationary points involved in the 32CA reaction of **AY11** and (E)-3,3,3-trifluoro-1-nitroprop-1-ene**10**calculated atMPWB1K/6-31G(d) level

System	ΔE (kcal/mol) Gas phase	ΔE (kcal/mol) Solvent
MC-mn	-9.89	-8.72
TS-mn	-4.75	-3.58
TS-mx	-2.38	-1.17
TS-on	-1.90	-0.61
TS-ox	-0.90	-0.06
CA-mn	-53.70	-51.89
CA-mx	-57.27	-55.35
CA-on	-55.28	-53.54
CA-ox	-52.49	-50.81

The electronic nature of the 32CA reaction of **AY11** with **FNP10** was evaluated using the computation of the GEDT[51]at the TSs corresponding to the four reaction paths. Along a polar reaction there is an electron-density transfer from the nucleophile to the electrophile, which can be analyzed through the GEDT value. Note that the larger GEDT at the TSs indicates the greater polarity of the reaction. However, cycloadditions with GEDT values below 0.05e correspond to non-polar processes whereas values higher than 0.2e correspond to polar processes. [52, 53] The natural atomic charges are obtained through a natural population analysis of the residual charge on the **AY11**. The positive values are indicative that electron flow takes place from **AY11** toward **FNP10**. The values of the GEDT computed are 0.22e at **TS-mn**, 0.24e at **TS-mx**, 0.27e at **TS-ox**, and 0.22e at **TS-on** (see Figure 2). They emphasize the high polar character of this 32CA reaction. These high GEDT values justify the computed low activation energies that are a consequence of the strong nucleophilicity value of **AY11** and the high electrophilicity index of **FNP10**.

Table 3. Relative[a] enthalpies (ΔH, in kcal/mol), entropies (ΔS in cal/mol · K), and Gibbs free energies (ΔG, in kcal/mol), at 308K. TSs involved in the studied 32CA reaction between **AY11** and trifluoronitropropene **10** calculated using MPWB1K/6-31G(d)level.

System	ΔH (kcal/mol)	ΔS (cal/mol·K)	ΔG (kcal/mol)
MC-mn	-6.22	62.06	7.06
TS-mn	-1.51	53.00	14.55
TS-mx	0.31	57.91	14.87
TS-on	1.03	56.36	16.06
TS-ox	2.02	53.55	17.91
CA-mn	-48.17	59.58	-34.13
CA-mx	-51.35	55.11	-35.84
CA-on	-49.35	55.56	-31.77
CA-ox	-46.81	56.33	-31.77

[a] *relative to [AY**11**+ alkene**10**]*

To investigate how thermal corrections can modify the relative electronic energies and selectivities, further calculations of thermodynamic properties in benzene at 308 k and 1 atm were performed on the 32CA reaction between **AY11** and alkene **10**. Thus, the obtained values of relative enthalpies, entropies, Gibbs free energies and the relative ones are given in Table 3, while the total ones are given in Table S4 in SI.

We can notice that the inclusion of thermal corrections to the electronic energies in benzene increases the relative enthalpies between 1.47 and 4.19 kcal/mol, thus, the relative activation enthalpies related to the TSs increase only by between 1.48 and 2.08 kcal/mol, in which the TS- mn remains more stable than TS-on by 1.82 kcal/mol. The addition of the entropic contribution to enthalpies increases the Gibbs free energies to 14.55, 14.87, 16.06, and 17.91 kcal/mol for TS-mn, TS-mx, TS-on, and TS-ox, respectively, as a consequence of the unfavorable activation entropy associated with these bimolecular processes, which are found in the range -34.13 and -31.77 kcal/mol, and making the possibility to classify this 32CA reaction as a strongly exergonic and irreversible reaction. while the formation of CA-mn remains exergonic by -35.34 kcal·mol^{-1}; consequently, this later is formed by kinetic control.

The geometries of the optimized TSs associated with the 32CA reaction of **AY11** with **FNP10** are shown in Figure 2. For the *meta* TSs, the lengths of the C1−C4 and C3−C5 new single bond are 2.219, 2.569Å at **TS-mn** and 2.245, 2.504Å at **TS-mx**, respectively. At the *ortho*

TSs, the lengths of the C1−C5 and C3−C4 are 2.352, 2.252 Å at **TS-on,** and 2.264, 2.388Å at **TS-ox**. From these geometrical parameters, the distance between the two C1 and C4 interacting carbon atoms indicate that the more favorable *meta* TSs are geometrically asynchronous, while for the *ortho* ones are slightly asynchronous. Interestingly, the most favorable **TS-mn** is slightly more asynchronous than the **TS-mx**. In addition, at the *meta* TSs, the formation of the C1−C4, the newly σ bond is clearly shorter than the C3−C5. Therefore, an asynchronous bond formation process in which the C1−C5 bond formation is more advanced than the C3–C4 one can be expected along the more favorable *meta* regio-isomeric pathways.

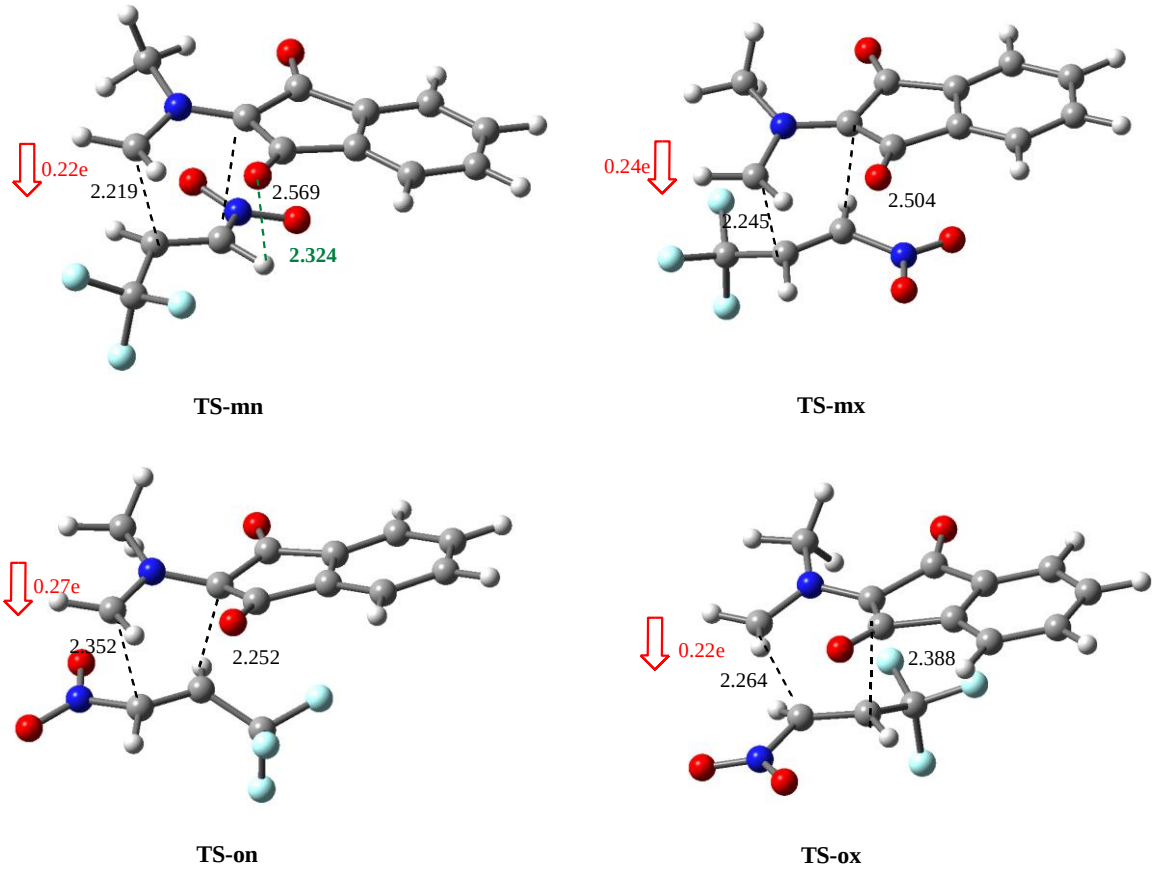

Figure 2. Optimized geometries of the TSs associated with the 32CA reaction between **AY11** and **FNP10** including the lengths of the new forming bonds in Å together with the values of the GEDT (in red). Hydrogen-bonds are indicated in green dotted line

4. ELF ANALYSIS

In this part, we focus on investigating the nature of the molecular mechanism of this 32CA reaction. Thus, recently, Domingo *et al.*[54] explain the reaction mechanism in highly

asynchronous single-bond formation processes, in which they have defined the concept of *two-stage one-step* mechanism, in which they suggest that the formation of the two single bonds takes place in two clearly differentiated stages of a one-step mechanism. This definition, which focuses only on the formation of the two single bonds, clearly indicates that the bonding changes in such one-step reactions are non-concerted processes. [55] In contrast of non-concerted processes, the concerted mechanism presents a single apparent transition state but is composed of several primitive processes (model proposed by Labet and co-workes). [56]

In order to understand well, the molecular mechanism of the studied 32CA along the reaction path, an ELF topological analysis of the reagents **AY11**and **FNP10** was performed. Afterwards, an ELF analysis of six relevant points along the IRC profile, associated with the formation of the two new C–C single bonds, were selected and analyzed for the more favorable pathway (see Figure 3).

As shown in Figure 3, the most significant basins are those corresponding to the interacting systems in both **AY11** and **FNP10** that are the C1–N2, N2–C3, and C4–C5 bonds. In the **AY11** system, the C1−N2 bonding region of **AY11** is characterized by a V(C1, N2) disynaptic basin with a population of 3.44e. On the other hand, the N2–C3 bonding region of **AY11** is characterized by the presence of one V(N2, C3) disynaptic basin with a population of 2.20e. Also, the presence of two monosynaptic V(C3) and V'(C3) basins on C3 with a population of 0.48e for each one, characterize the C3 as a pseudoradical centre.[57] It is worth noting that the sum of the V(C1,N2) and the disynaptic basins population of 3.44e is very close to the 4e present in the C1–N2 double bond region of the Lewis structure of **AY11**. Note that in the **FNP10**, the C4–C5 double bond is characterized by the presence of two disynaptic basins, V(C4,C5) and V'(C4,C5), with a population of 1.78e for each one (see Figure3).

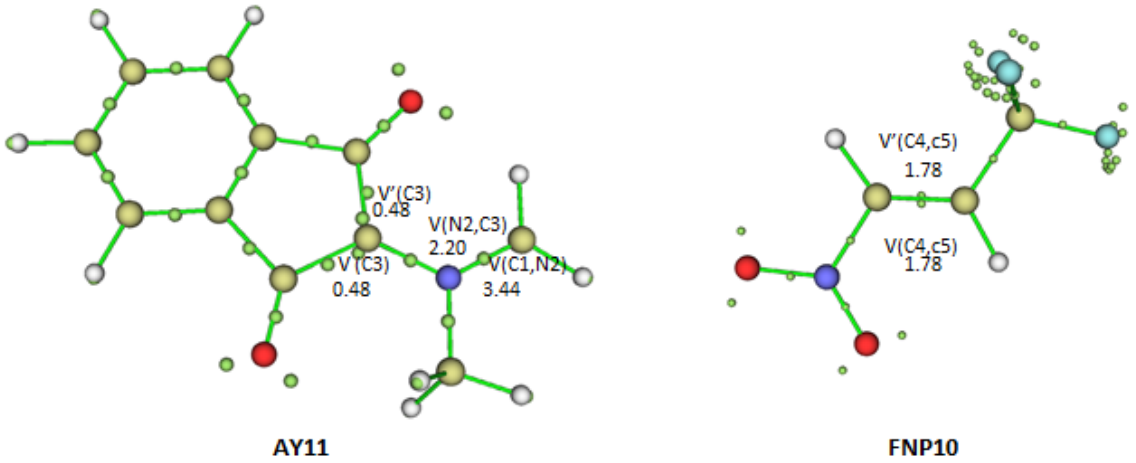

Figure 3. Electron localization function attractor positions for the reagents **FNP10** and **AY11** in the ground states together with the electronic populations of reactive valence basins

The ELF attractors and populations of the most significant valence basins for the selected point along the *meta/endo* reactive channel of the cycloaddition reaction between **AY11** and **FNP10** are given in Figure 4.

The first selected point from the IRC path is the molecular complex (**MC**) which is stabilized by electrostatic interactions. At this structure, the two interacting fragments are very far apart (with d(C1−C4) = 3.16 Å and d(C3−C5) = 3.03Å). Thus, except for slight changes in electron density in this system, ELF topology was found similar to that found in the separated reagents. In this regard, the main population changes occur at the C1–N2 bonding region of **AY11**, represented at **MC** by the V(C1,N2) and V'(C1,N2) disynaptic basins with 3.40e of population, which accounts for a C1=N2 double bond. In addition, the N2−C3 region is characterized by the presence of V(N2,C3) disynaptic basin with a population of 2.22e. On the other hand, the C4–C5 double bond in **AY11** is characterized by the presence of two disynaptic basins, V(C4,C5), V'(C4,C5), that are characterized by a slight different of population values, 1.75 and 1.79e, respectively.

The most relevant feature of TS-on is the creation of a new V(C3) monosynaptic basin integrating 0.49 e, while the V(C1) monosynaptic basins present at MC-on is slightly depopulated to 0.29 e. This new monosynaptic basin, which is created at the second most nucleophilic center of AY 21 (see Parr functions in Figure 2), is demanded for the subsequent creation of the first new C3–C4 single bond [26]. On the other hand, the two disynaptic basins associated with the C4–C5 partial double bond present at ferrocene ethylene 22 and MC-on merge into one single V(C4–C5) disynaptic basin at TS-on after losing 0.71 e from ethylene 22. This ELF analysis of TS-on, which accounts for the non-concerted nature of this one-step 32CA reaction, supports the previous analysis based on the geometrical param

At the transition state **TS-mn**, where, d(C1–C4)=2.22 Å and d(C3–C5)=2.57 Å, two monosynaptic basins appear at the C1 and C3 carbon atoms of **AY11** with an initial population of 0.26e and 0.41e, respectively, characterize the C1 and C3 as a pseudodiracal center; and responsible of the pseudodiradical behavior of **AY11** [57] which accounts for the slight depopulation of the double C1–N2 bond that becomes 3.18e, which was 3.40e at the **MC** point. This depopulation is due to the preparation of the formation of the two new bondsC1–C4 and C3–C5. Moreover, the double bond C4−C5 of the trifluoro-nitro-propene **10** has been also populated with three similar disynaptic basins, with 3.53e of electronic population for each one.

At the first point after **TS-mn**, named **P1**, where dC1–C4)= 1.96 Å and d(C3–C5) =2.65Å, the double C1=N2 is characterized by a V(C1,N2) disynaptic basin; its electron density is slightly depopulated from 3.18 to 2.16, due to the high electron donating character of **AY11**. The presence of two disynaptic basins V(C1,C4) and V' (C1,C4), integrating 1.14e, is an indicator for a very early initiated formation of C1–C4 σ bond, which accounts for the non-concerted nature of this one-step 32CA reaction. Furthermore, the **FNP10** system fragment becomes characterized by a V(C4–C5) disynaptic basin and depopulated to 2.70e.

At the **P2** point,where d(C1–C4)=1.58Å and d(C3–C5)=1.95Å,the two V(C1) and V(C4) monosynaptic basins that was created at **P1** point have merged into a new V(C1,C4) monosynaptic basin integrating 1.75e. This topological change indicates that the formation of the first C1–C4 single bond has already begun at a C1–C4 distance of 1.96Å through the C–C coupling of the C1 *pseudoradical* centers and C4 present in **P1** structure**.** At the same time, the two V(C3) and V(C5) monosynaptic basins presents in P1 have merged into a new V(C3,C5) disynaptic basin integrating 1.41e of population, respectively, together with a

decreasing in the population of the V(C4,C5) basin by 0.62e. This topological change indicates that the formation of the second C3–C5 σ bond begins when the first single C1–C4 bond is already formed.

At the **P3** point which is the last point in the IRC path before the *meta* cycloadduct, where d(C1–C4) =1.55 Å and d(C3–C5) =1.62 Å, we can notice the emergence of the two V(C3) and V(C5) monosynaptic basins in a new single V(C3,C5) disynaptic basin integrating 1.76e, indicating that the beginning of C3–C4 single bond formation starts at a distance of 1.95 Å. In the same way, the population of the V(C1,C4) disynaptic basin related to the C1−C4 single bond remains 1.82e. This topological change indicates that the formation of the second C3–C5 single bond begins when the C1–C4 single bond is formed by more than 94% through the merger of the electron density of the C3 and C5 *pseudoradical* centers. On the other hand, we notice that the V(N2,C3) disynaptic basin is depopulated by 0.61e at **P3** point in comparison with its population at **P2** point.

As a result, this ELF topological analysis focused on the formation of the C1–C4 and C3–C5 single bonds establishes that this 32CA reaction takes place through a *two-stage one-step* mechanism in which the formation of the second C1−C4 single bond begins when the first C3−C5 single bond is 94% formed, accounting for a non-concerted mechanism.[52] Thus, the presence of the pseudoradical C3 at the **AY11**, categorizes this TAC as a pseudo(mono)radical TAC in this pdr-type 32CA reaction of **AY11**.[52]

Table 4. Electronic populations of valence basin obtained from ELF analysis of the selected points associated with 32CA reaction between **AY11** and **FNP10**.Distances are given in angstroms (Å), electron populations are given in average number of electrons, e

	MC	**TSmn**	**P1**	**P2**	**P3**	**CA-mn**
d(C1-C4)	3.16	2.22	1.96	1.58	1.55	1.52
d(C3-C5)	3.03	2.57	2.65	1.95	1.62	1.53
V(C1,N2)	3.40	3.18	2.16	1.70	1.69	1.71
V(N2,C3)	2.21	2.34	2.51	2.01	1.78	1.67
V(C4,C5)	1.79 1.75	3.53 3.53 3.53	2.70	2.08	1.98	1.94
V(C1)	-	0.26	-	-	-	-
V(C1,C4)	-	-	1.14-1.14	1.75	1.82	1.85
V(C3)	-	0.41	0.33	-	-	-

V(C5)	-	-	0.40	-	-	-
V(C3,C5)	-	-	-	1.41	1.76	1.93

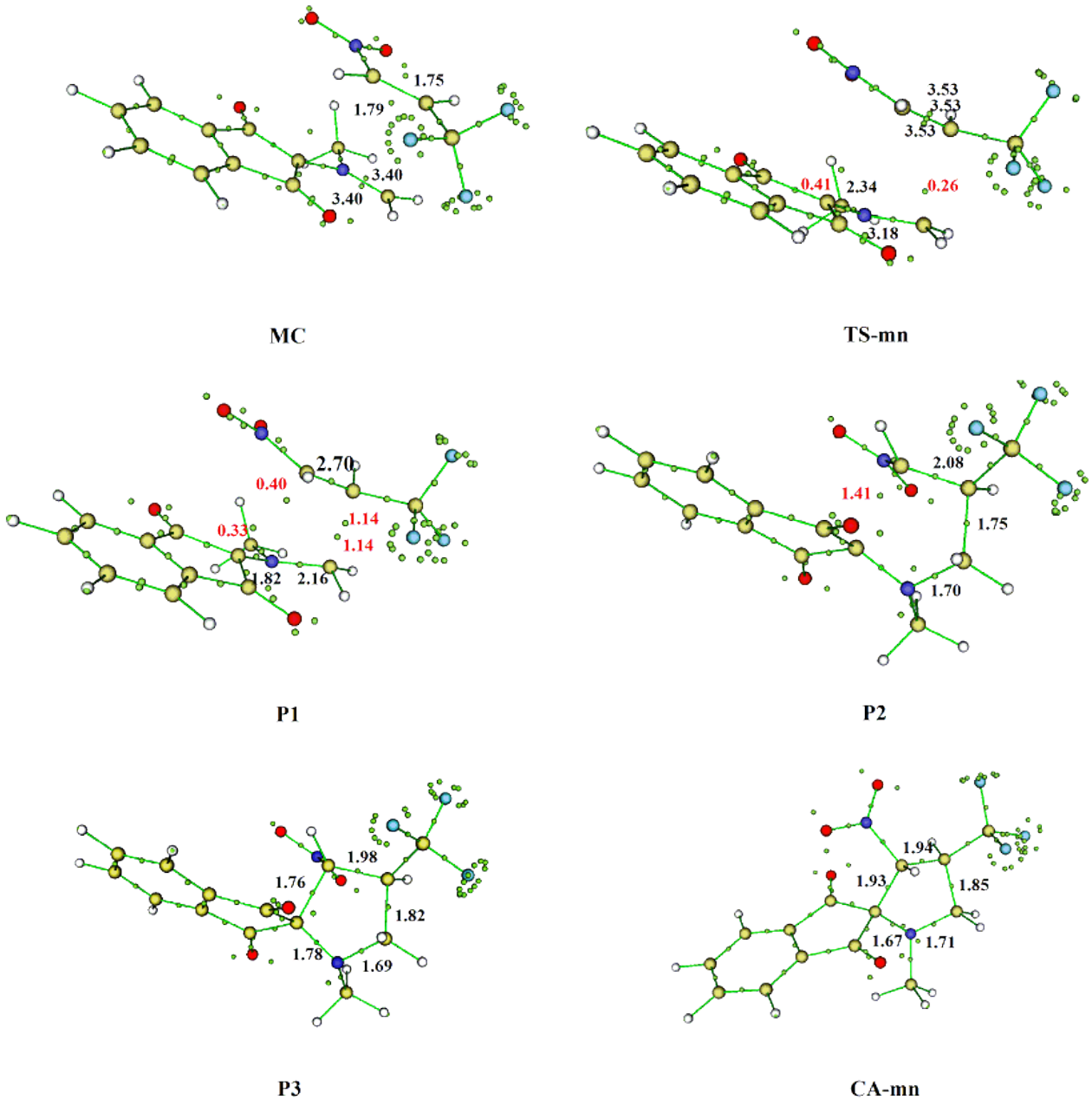

Figure 4. ELF attractors and populations of the most significant valence basins for the selected point along the meta/endo reactive channel of the 32CA reaction between **AY11** and **FNP10**

5. Origin of the *meta/endo* selectivity

5. 1 NCI analysis

As proved in the previous section, the 32CA reaction of azomethine ylide**AY11** with trifluoronitropropene **FNP10** yields the pyrrolidine **CA-mn**, resulting from the *meta/endo* approach mode. Thus, numerous theoretical studies confirm that the high selectivity approach are generally governed by covalent and non-covalent interactions.[58] For the goal to obtain a deep insight into these behaviors, we have performed a NCI analysis on the structures of the more favoured transition states, **TS-mn** and **TS-mx**.

As seen in Figure 5, the most significant difference in both TSs is the presence of a larger green surface between the azomethine ylide **AY11**and trifluoronitropropene **FNP10** in the *endo* TS in comparison with that in the *exo* one. This larger green surface, associated with weak attractive van der Waals interactions, accounts for a significant stabilization of the *endo* approach (**TS-mn**). In addition, both TSs structures present two blue circle areas situated in the C–C new forming σ bond regions, in which the darkness in the blue color accounts for the asynchronicity in the bond formation processes. Also, we can see that the new σ bond formation involving the most electrophilic C4 center of trifluoronitropropene **FNP10** is more advanced than the second σ bond involving C5 center. Furthermore, the NCI surfaces of **TS-mn** show the presence of two crucial colored area varied between green and turquoise colors which indicate, therefore, the presence of several HBs interactions such as H…N and H…F one. Note that the analysis of the optimized structure of **TS-mn** (Figure 2) reveals also the possible presence of one weak hydrogen bond which can be developed between one hydrogen of the methyl group of azomethine ylide framework and the oxygen atom of the nitro group of the **FNP10**, in which this O…H distance is 2.324 Å (Figure 2). Consequently, these conventional interactions enhance the stability of the **TS-mn** over **TS-mx** one.

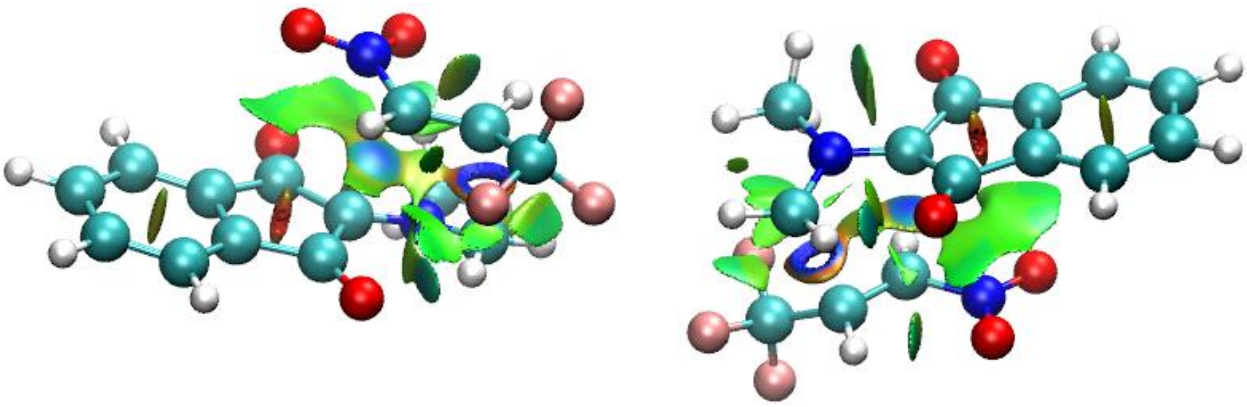

TS-mn **TS-mx**

Figure 5. Favorable non-covalent interaction (**NCI**) gradient isosurfaces of **TS-mn** and **TS-mx** structures involved in the 32CA reaction of **AY11** with **FNP10**

5. 2 QTAIM analysis

Nowadays, the quantum theory of atoms in molecules (QTAIM) appears as one of the powerful tools to describe the nature of molecular interactions.[59] The fundamental concept of QTAIM theory is based on the analysis of the electron density ρ which provides by series of critical points such as (3, +3), (3, -3), (3, +1), and (3, -1) (cp) between atoms of the molecular system; the (3, -1) are the most essential points which are associated with the existence of a stabilization interaction, namely, a hydrogen bond (HB). [60] This theory offers an elegant approach to unraveling the intermolecular interactions based on the values obtained by the ρ_{bcp} and $\nabla^2\rho_{bcp}$[61] Recently, Rosas *et al.* [60] classify HBs interactions according to three types, primary the strong HBs are characterized by a Laplacian, $\nabla^2\rho_{bcp} < 0$ and a total electron energy density, $H_{bcp} < 0$, a medium strength HBs are characterized by a, $\nabla^2\rho_{bcp} < 0$ and $H_{bcp} > 0$, finally weak strength HBs are defined by, $\nabla^2\rho_{bcp} > 0$ and $H_{bcp} > 0$.

In order to confirm the presence of the non-covalent interactions, QTAIM analysis of the electron density was performed at the critical points for the favourable **TS-mn**. The QTAIM parameters of the (3, -1) critical points (cps) of **TS-mn** are collected in Table 5, while the corresponding molecular graphs together with pcb numbering at **TS-mn** obtained by QTAIM analysis of electron density at MPWB1K/6-31G(d) theoretical level is represented in Figure 6.

Table 5 displays the presence of six critical bcp points, in which there are two strong interactions characterized by negative H_{bcp}values (H_{bcp}=-0.125) and (H_{bcp}=-0.168) associated

with the formation of new forming bonds C1−C4 and C3−C5 respectively. In addition, the positive sign of Laplacian ($\nabla^2\rho_{bcp}$> 0) and electron energy density (H_{bcp}> 0) of the four other (3, -1) bcp, allow us to classify them as weak stabilized conventional and non-conventional HB.On the other side, the QTAIM graphs displays two intramolecular interactions (C…O and O…H), in which C…O interaction may be classified as a weak non-conventional stabilized HBs with $\nabla^2\rho_{cbcp}$=0.591 and H_{bcp}= 0.172, together with weak conventional O…H interaction characterized by $\nabla^2\rho_{cbcp}$=0.831and H_{bcp}= 0.393.On the other hand, we notice the presence of a conventional stabilized O…H HB (since it occurs between oxygen atom of nitro group and hydrogen atom of methyl group) and a non-conventionl C…F (bcp n°41) characterized also by $\nabla^2_{\rho bcp}$>0 and H_{bcp}>0, which may be classified as weak interactions.Therefore, these important number of HBs present at **TS-mn**, enhance the stability of *meta-endo* approach and contribute in the formation favoring of **CA-mn**.

Table 5. QTAIM parameters (in a.u.) of the (3, -1) bond critical points presented in **TS-mn**

Interaction	**bcp label**	ρ_{bcp}	$\nabla^2\rho_{bcp}$	H_{bcp}
C1···C4 (new bond)	63	0.563	0.481	-0.125
C3···C5(new bond)	58	0.312	0.567	-0.168
C···F	41	0.620	0.304	0.102
O···H–C	73	0.123	0.467	0.987
H···**O (intra)**	50	0.236	0.831	0.393
O···C (intra)	75	0.146	0.591	0.172

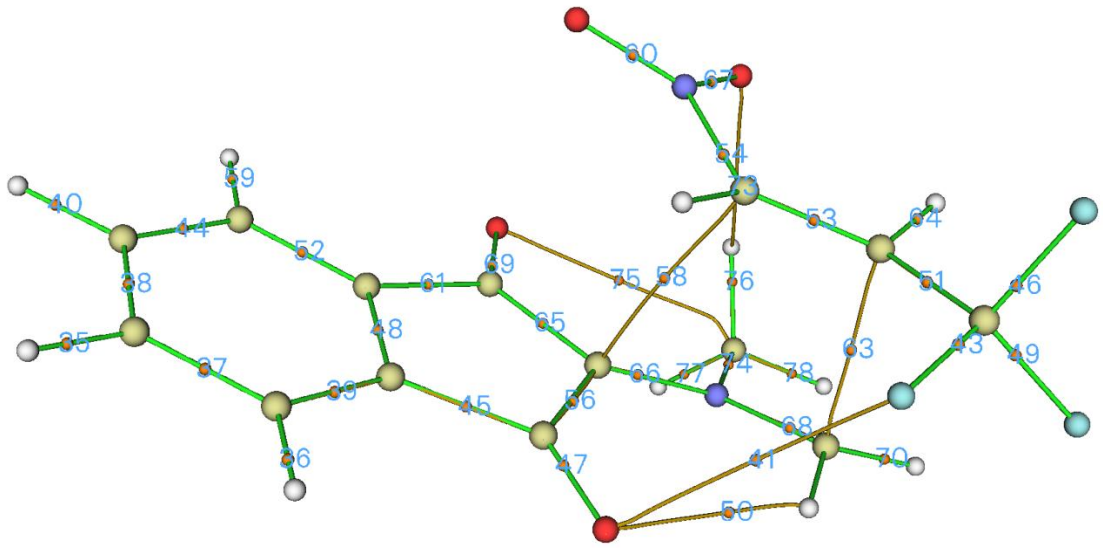

Figure 6. Molecular graphs of **TS-mn** obtained by QTAIM analysis of MPWB1K/6-31G(d) electron density, with (3, -1) critical points (orange sphere) bond paths (brown lines), together with the numbering of relevant (3, -1) bcp points

6. CONCLUSIONS

The molecular mechanism and the regio- and stereoselectivity of the 32CA reactions of **AY11** with alkene**FNP10** have been investigated within MEDT using DFT methods at the MPWB1K/6-31G(d) level. Four reactive channels associated with the *meta*/*ortho* regio- and *endo*/*exo* stereoselective approach modes have been explored and characterized. The following conclusions can be drawn from the obtained results:

- This 32CA reaction take place with a very low activation energy.
- This 32CA reaction is completely *meta* regioselective with high *endo* stereoselectivity in agreement with the experimental results.
- The solvent effects were also considered which do not produce any markedly change relative to the gas phase regio and streoselectivity.
- The high GEDT values computed at the TSs emphasize the high-polar character of this 32CA reaction, in agreement with the strong nucleophilic character of **AY11** and strong electrophile character of **FNP10**.
- ELF topological analysis focused on the formation of the C_1–C_4 and C_3–C_5 single bonds along the *meta*/*endo* reaction pathway allows establishing correctly that this 32CA reaction of **AY11** with **FNP10**proceeds *via* a non-concerted *two-stage one-step*

mechanism in which the formation of the second C_3–C_5 single bond begins when the first C_1–C_4 single bond is 94% formed.

- NCI and QTAIM analyses revealed that the presence of several types of non-covalent interactions accountable for the *meta-endo* stability.

ACKNOWLEDGMENTS

This work was supported by the Ministry of Higher Education and Scientific Research of the Algerian Government [projects PRFU Code: A6N0UN202090005].The GENCI/CINES (Project cpt2130) and the PSMN of the ENS-Lyon are acknowledged for HPC resources/computer time.

CONFLICT OF INTEREST

The authors declare no conflict of interest.

REFERENCES

[1] Seo T S, Bai X, Ruparel H, Li Z, Turro NJ, Ju J, (2004) Photocleavable fluorescent nucleotides for DNA sequencing on a chip constructed by site-specific coupling chemistry. *Proc, Natl. Acad. Sci. U. S.* A101, 5488

[2] SpeersA E, Adam GC, Cravatt BF (2003)Activity-based protein profiling in vivo using a copper (i)-catalyzed azide-alkyne [3+ 2] cycloaddition. *J Am Chem Soc* 125 (16):4686–4687

[3] Krasinski A, Radic Z, Manetsch R, Raushel J, Taylor P, Sharpless KB, Kolb H, Kolb C (2005)In Situ Selection of Lead Compounds by Click Chemistry: Target-Guided Optimization of Acetylcholinesterase Inhibitors. *J Am Chem Soc* 127(18):6686–6692

[4] Ríos-Gutiérrez M, Domingo Luis R., Unravelling the Mysteries of the [3+2] Cycloaddition ReactionsEur. *J. Org. Chem.* 2019, 267-282

[5] Franchetti P, Marchetti LS, Cappaellaci JA, Yalowitz HN, Jayaram BM, Glodstein M, Grafantini A (2001)A new C-nucleoside analogue of tiazofurin: synthesis and biological evaluation of 2-β-d-ribofuranosylimidazole-4-carboxamide (imidazofurin).*Bioorg Med Chem Lett* 11(1):67-69

[6] Kocabaş E, Sarıgüney A B, Erci F, Çakır-Koç R, Kocabaş Hilal Ö, Emrah Torlak, Ahmet Coşkun, (2011)Synthesis, Antibacterial and Cytotoxic Activities of New Thiazole Based Pyrrolidine Derivatives.*Biointerface Research in Applied Chemistry* 11, 12178 -12185

[7] Schwartz JC. (2011)The histamine H3 receptor: from discovery to clinical trials with pitolisant. *British J Pharmacology* 163(4):713-721

[8] Schramm S, Köhler N and Rozhon W, (2019)Pyrrolizidine Alkaloids: Biosynthesis, Biological Activities and Occurrence in Crop Plants. *Molecules24*: 498-541

[9] Prabhakaran P and Rajakumar P (2020)Regio- and stereoselective synthesis ofspiropyrrolidine-oxindole and bis-spiropyrrolizidine-oxindole grafted macrocycles through [3 + 2] cycloaddition of azomethine ylides.*RSC Adv* 10 : 10263-10276

[10] Boudriga S, Haddad S, Murugaiyah V, Askr M, Knorr M, Strohmann C, Golz C (2020) Three-Component Access to Functionalized Spiropyrrolidine Heterocyclic Scaffolds and Their Cholinesterase Inhibitory Activity. *Molecules 25*(8) 1963-1984

[11] Domingo LR, Kula K, Ríos-Gutiérrez M (2020)Unveiling the Reactivity of Cyclic Azomethine Ylides in [3+2] Cycloaddition Reactions within the Molecular Electron Density Theory. *Eur J Org Chem*5938–5948.

[12] Nasri L, M. Rios-Gutierrez, Nacereddine AK, Djerourou A, Domingo LR (2017) A molecular electron density theory study of [3 + 2] cycloaddition reactions of chiral azomethine ylides with β-nitrostyrene.*Theor Chem Acc* 136 (9):104

[13] Hussein EM, El Guesmi N, Moussa Z, Uttam P, Samir K P, Dasgupta T, Ahmed SA(2020) Unprecedented Regio- and Stereoselective Synthesis of Pyrene-Grafted Dispiro[indoline-3,2′-pyrrolidine-3′,3″-indolines]: Expedient Experimental and Theoretical Insights into Polar [3 + 2]Cycloaddition. *ACS Omega* 5(37):24081–24094

[14] Wang X, Zhang Y, Yang Y, Xue Y (2020) Mechanism and Diastereoselectivity in Formation of Trifluoromethyl-Containing Spiro[pyrrolidin-3,2'-oxindole] by a Catalyst-free and Mutually Activated [3+2]-Cycloaddition Reaction: A Theoretical study. *New Journal of Chemistry* 44(40):17465-17476

[15] Alexey Yu. Barkov, Nikolay S. Zimnitskiy, Igor B. Kutyashev, Vladislav Yu. Korotaev(2017)Highly regio- and stereoselective 1,3-dipolar cycloaddition of stabilised azomethine ylides to 3,3,3-trihalogeno-1-nitropropenes: synthesis of trihalomethylated spiroindenepyrroli(zi)dines.*Journal of Fluorine Chemistry* 204:37–44

[16] HoukKN, SimsJ, DukeRE, StrozierRW, GeorgeJK(1973) Frontier molecular orbitals of 1,3dipolesanddipolarophiles. *J. Am. Chem.Soc* 95 :7287–7301

[17] DomingoLR, Ríos-Gutiérrez M, Pérez P (2017) How does the global electron density transferdiminishactivation energies in polar cycloaddition reactions? A Molecular Electron Density Theorystudy *Tetrahedron*, 73: 1718–1724

[18] Sobhi C, Nacereddine AK, Djerourou A, Ríos-Gutiérrez M, Domingo LR (2017) A DFT study of the mechanism and selectivities of the [3+ 2] cycloaddition reaction between 3-(benzylideneamino) oxindole and trans-β-nitrostyrene. *J Phys Org Chem* 30(6):e3637

[19] ZhaoY, Truhlar DG, (2004) Hybrid Meta Density Functional Theory Methods for Thermochemistry, Thermochemical Kinetics, and Noncovalent Interactions: The MPW1B95 and MPWB1K Models and Comparative Assessments for Hydrogen Bonding and van der Waals Interactions. *J Phys Chem A* 108 (33): 6908–6918

[20] Hehre WJ, Radom L, Schleyer PVR, Pople JA (1986) Ab Initio molecular orbital theory. Wiley, New York 9 : 399–406

[21] Ríos-Gutiérrez M, Chafaa F, Nacereddine AK, Djerourou A, Domingo LR (2016) A DFT study of [3+2] cycloaddition reactions of an azomethine imine with N-vinyl pyrrole and N-vinyl tetrahydroindole. *Journal of Molecular Graphics and Modelling*70:296-304

[22] Schlegel HB (1982) Optimization of equilibrium geometries and transition structures. *J Comput Chem* 3(2):214–218

[23] Fukui K (1970) Formulation of the reaction coordinate. *J Phys Chem* 74: 4161 –4163

[24] Gonzalez C, Schlegel HB (1990) Reaction path following in mass-weighted internal coordinates. *J Phys Chem* 94: 5523–5527; Gonzalez C, Schlegel H B (1991) Improved algorithms for reaction path following: Higher-order implicit algorithms. *J Chem Phys* 95: 5853

[25] Tomasi J, Persico M (1994) Molecular interactions in solution: an overview of methods based on continuous distributions of the solvent. *Chem Rev* 94:2027; Simkin BY, Sheikhet I (1995) Quantum chemical and statistical theory of solutions—computational approach. Ellis Horwood, London

[26] Cances E, Mennucci B, Tomasi J (1997) A new integral equation formalism for the polarizable continuum model: theoretical background and applications to isotropic and anisotropic dielectrics. *J Chem Phys* 107:3032;
[27] Cossi M, Barone V, Cammi R, Tomasi J (1996) Ab initio study of solvated molecules: a new implementation of the polarizable continuum model. *Chem Phys Lett* 255:327;
[28] Barone V, Cossi M, Tomasi J (1998) Geometry optimization of molecular structures in solution by the polarizable continuum model. *J Comput Chem* 19:404
[29] Becke AD (1993) Density-functional thermochemistry. III. The role of exact exchange. *J Chem Phys* 98:5648
[30] Scott A Pand Radom L (1996) Harmonic Vibrational Frequencies: An Evaluation of Hartree−Fock, Møller−Plesset, Quadratic Configuration Interaction, Density Functional Theory, and Semiempirical Scale Factors *J Phys Chem*100 (41): 16502–16513
[31] Domingo LR (2014) A new C–C bond formation model based on the quantum chemical topology of electron density. *RSC Adv* 4: 32415–32428
[32] Becke AD, Edgecombe KE (1990) A simple measure of electron localization in atomic and molecular systems. *J Chem Phys* 92:5397–5403
[33] Lu T, Chen F (2012) Multiwfn: a multifunctional wavefunction analyzer. *J Comput Chem* 33:580
[34] Frisch MJ, Trucks GW, Schlegel HB, Scuseria GE, Robb MA, Cheeseman JR, Scalmani G, Barone V, Mennucci B, Petersson GA, Nakatsuji H, Caricato M, Li X, Hratchian HP, Izmaylov AF, Bloino J, Zheng G, Sonnenberg JL, Hada M, Ehara M, Toyota K, Fukuda R, Hasegawa J, Ishida M, Nakajima T, Honda Y, Kitao O, Nakai H, Vreven T, Montgomery JA, Peralta JE, OgliaroJr F, Bearpark M, Heyd JJ, Brothers E, Kudin KN, Staroverov VN, Kobayashi R, Normand J, Raghavachari K, Rendell A, Burant JC, Iyengar SS, Tomasi J, Cossi M, Rega N, Millam JM, Klene M, Knox JE, Cross JB, Bakken V, Adamo C, Jaramillo J, Gomperts R, Stratmann RE, Yazyev O, Austin AJ, Cammi R, Pomelli C, Ochterski JW, Martin RL, Morokuma K, Zakrzewski VG, Voth GA, Salvador P, Dannenberg JJ, Dapprich S, Daniels AD, Farkas O, Foresman JB, Ortiz JV, Cioslowski J, Fox D (2009) Gaussian 09, Revision A.02. Gaussian, Wallingford
[35] Parr RG, von Szentpaly L, Liu S (1999) Electrophilicity index. *J Am Chem Soc* 121:1922
[36] Parr RG, Pearson RG (1983) Absolute hardness: companion parameter to absolute electronegativity. *J Am Chem Soc* 105:7512; Parr RG, Yang W (1989) Density functional theory of atoms and molecules. Oxford University Press, New York
[37] Chermette H (1999) Chemical reactivity indexes in density functional theory *J. Comput. Chem.* 20, 129-154
[38] Domingo LR, Chamorro E, Pérez P (2008) Understanding the reactivity of captodativeethylenes in polar cycloaddition reactions A theoretical study. J Org Chem 73:4615–4624; Domingo LR, Pérez LP (2011) The nucleophilicity N index in organic chemistry. *Org Biomol Chem* 9:7168–7175
[39] Kohn W, Sham LJ (1965) Self-consistent equations including exchange and correlation effects. *Phys Rev* 140:1133–1138
[40] Johnson ER, Keinan S, Mori-Sanchez P, Contreras-Garcia J, Cohen AJ, Yang W (2010) Revealing noncovalent interactions. *J Am Chem Soc* 132:6498
[41] Lane JR, Contreras-Garcia J, Piquemal JP, Miller BJ, Kjaergaard HG (2013) Are bond critical points really critical for hydrogen bonding? *J Chem Theory Comput* 9:3263
[42] Contreras-Garcia JE, Johnson R, Keinan S, Chaudret R, Piquemal JP, Beratan DN, Yang W (2011) NCIPLOT: a program for plotting noncovalent interaction regions. *J Chem Theory Comput* 7:625
[43] Bader RFW (1990) Atoms in molecules. A quantum theory. Clarendon press, Oxford

[44] Nacereddine AK, Sobhi C, Djerourou A, Ríos-Gutiérrez M, LR Domingo (2015) Non-classical CH...O hydrogen-bond determining the regio- and stereoselectivity in the [3 + 2] cycloaddition reaction of (Z)-C-phenyl-Nmethylnitrone with dimethyl benzylidene cyclopropane-1,1-dicarboxylate. A topological electron-density study. *RSC Adv* 5: 99299-99311

[45] Sobhi C, Nacereddine AK, Djerourou A, Aurell M J, and Domingo L R (2012) The role of the trifluoromethyl group in reactivity and selectivity in polar cycloaddition reactions. A DFT study *Tetrahedron*, 68: 8457-8462

[46] Domingo LR, Sáez JA (2009) Understanding the mechanism of polar Diels–Alder reactions. *Org Biomol Chem* 7*:*3576-*3583*

[47] Domingo LR, Ríos-Gutiérrez M, Pérez P (2020) A molecular electron density theory study of the participation of tetrazines in aza-Diels–Alder reactions. RSC Adv., 10, 15394

[48] Domingo LR, Aurell MJ, Pérez P, Contreras R (2002) Quantitative characterization of the global electrophilicity power of common diene/dienophile pairs in Diels-Alder reactions. *Tetrahedron* 58: 4417

[49] Jaramillo P, Domingo LR, Chamorro E, Pérez PJ (2008) A further exploration of a nucleophilicity index based on the gas-phase ionization potentials. J Mol Struct 865:68–72

[50] Benchouk W, Mekelleche SM, Silvi B, Aurell MJ, Domingo LR (2011) Understanding the kinetic solvent effects on the 1,3-dipolar cycloaddition of benzonitrile N-oxide: a DFT study. *J Phys Org. Chem* 24:611

[51] Hamza-Reguig S, Bentabed-Ababsa G, Domingo L R, Ríos-Gutiérrez M, Philippot S, Fontanay S, Duval E, Ruchaud S, Bach S, Roisnel T, Mongin F, *(*2017) A combined experimental and theoretical study of the thermal [3+2] cycloaddition of carbonyl ylides with activated alkenes.*J. Molec Struct* 1157:276−287

[52] Domingo LR, Saez JA, Zaragoza RJ, Arno M, (2008) Understanding the Participation of Quadricyclane as Nucleophile in Polar [2σ + 2σ + 2π] Cycloadditions toward Electrophilic π Molecules *J. Org. Chem* 73, 8791–8799

[53] Jasinski R, Mroz K, ącka A K (2016) Experimental and Theoretical DFT Study on Synthesis of Sterically Crowded 2,3,3,(4)5-Tetrasubstituted-4-nitroisoxazolidines via 1,3-Dipolar Cycloaddition Reactions Between Ketonitrones and Conjugated Nitroalkenes. *J Heterocycl Chem* 53:1424

[54] Domingo LR, Ríos-Gutiérrez M (2017) A Molecular Electron Density Theory Study of the Reactivity of Azomethine Imine in [3+2] Cycloaddition Reactions. *Molecules* (22): 750

[55] Ríos-Gutiérrez M, Darù A, Tejero T, Domingo L R and Merino P (2017) A molecular electron density theory study of the [3 + 2] cycloaddition reaction of nitrones with ketenes. *Org Biomol Chem* (15):1618

[56] Labet V, Morell C, Toro-Labbe A, Grand A (2010) Is anelementary reaction step reallyelementary? Theoretical decomposition of asynchronous concerted mechanisms. *Phys. Chem. Chem. Phys*., 12, 4142−4151

[57] Domingo LR, Sáez JA (2011) Understanding the Electronic Reorganization along the Nonpolar [3+ 2] Cycloaddition Reactions of Carbonyl Ylides. *J. Org. Chem*., 76, 373–379

[58] Rozenberg M (2014) The hydrogen bond – practice and QTAIM theory. *RSC Adv*., 26928−26931

[59] Chouit H, Sobhi C, Bouasla S, Messikh S, Kheribeche A, Nacereddine AK (2022) Effect of hydrogen bonds and CF3 group on the regioselectivity and mechanism of [3+2] cycloaddition reactions between nitrile oxide and2,4-disubstitutedcyclopentenes. A MEDT stud. *Journal of Molecular Modeling* 28: 104

[60] Rozas I, Alkorta I, Elguero J (2000) Behavior of Ylides Containing N, O, and C Atoms as Hydrogen Bond Acceptors *J. Am. Chem. Soc*122(45):11154–1116

[61] Shyam Vinod Kumar P, Raghavendra V and Subramanian V (2016) Bader's Theory of Atoms in Molecules (AIM) and its Applications to Chemical Bonding *J. Chem. Sci.* 128, 1527–1536